Physics Open 4 (2020) 100026

Contents lists available at ScienceDirect

Physics Open

journal homepage: www.journals.elsevier.com/physics-open

A capacitor dosimeter with disposable silicon-diode substrates for 4-MV X-ray beam detection in radiation therapy

Satoshi Yamaguchi [a,*], Eiichi Sato [b], Yoshiro Ieko [c], Hisanori Ariga [c], Kunihiro Yoshioka [a]

[a] Department of Radiology, School of Medicine, Iwate Medical University, 2-1-1 Idaidori, Yahaba, Iwate, 028-3695, Japan
[b] Department of Physics, Iwate Medical University, 1-1-1 Idaidori, Yahaba, Iwate, 028-3694, Japan
[c] Department of Radiation Oncology, Iwate Medical University Hospital, Iwate Medical University, 2-1-1 Idaidori, Yahaba, Iwate, 028-3695, Japan

ARTICLE INFO

Keywords:
Radiation dosimeters
Radiation monitoring
Cataract
Surface dose
Radiotherapy
Semiconductors

ABSTRACT

To monitor patient-surface dose in intensity-modulated radiation therapy (IMRT), developed a novel capacitor dosimeter with a disposable USB-A mini-substrate consisting of a 0.22 μF capacitor and a silicon X-ray diode (Si-XD). The capacitor dosimeter consisted of a USB-A mini-substrate and a microcomputer dock. The capacitor in the substrate was charged to 3.30 V using the dock before 4 MV X-ray irradiation. The charging voltage was reduced by photocurrents flowing through the Si-XD during irradiation. After which the substrate was re-inserted into the dock, and the discharging voltage was measured. A Farmer-type ionization chamber (N30013, PTW) was used to convert the discharging voltages into absorbed dose (Gy). The IMRT study was performed using a custom-made head-neck phantom. The decrease in the charging voltage was found to be proportional to the X-ray dose, and the calibrated dose corresponded well to those obtained using the ionization chamber. The surface dose measured on the head-neck phantom were equivalent to those obtained from a treatment planning system. An inexpensive dosimeter with Si-XDs was developed, as a promising too. The results suggest for monitoring patient-surface dose during radiation therapy.

1. Introduction

Ionization chambers are widely used to measure the absorbed dose in radiation therapy. However, these chambers do not to monitor patient-surface dose, which tend increase due to tumor shrinkage or weight loss during therapy, and cause radiation damage to the skin [1–5]. Monitoring patient-surface dose is, therefore, required. Furthermore, the influence of scattered radiation outside the irradiation field during therapy is not well understood. Measurement of the surface dose outside the field might be useful for monitoring cataract development in head-neck treatment [6,7]. Several detectors are used to measure surface dose during therapy, such as optically stimulated detectors, thermoluminescent dosimeters and radiochromic films. However, such dosimeters are not as precise as those of commercially available ionization chambers [8] and take relatively high cost. To monitor patient-surface dose during radiation therapy, it is desirable to use a low-priced detector that can show the results immediately.

Therefore, we have recently developed a low-priced capacitor dosimeter incorporating a disposable USB-A mini-substrate with a capacitor, and a silicon X-ray diode (Si-XD), which no needed cable connection for dose measurement.

A preliminary study with industrial X-ray tube with low-energy X-ray range was carried out and the result shows the decrease in the charging voltage was proportional to the delivered dose [9,10]. The Si-XD detector can also be used at high energy X-ray ranges, since scattered-low-energy photons are produced by the ceramic substrate behind the Si and detected by the Si diode [11].

In this study, we aim to conduct a feasibility study to monitor the patient's surface dose in radiation therapy using the developed capacitor dosimeter and a medical linear accelerator (linac). A 4-MV X-ray beam from a linac was used measure the surface dose with this capacitor delivered to custom-made head-neck phantom. A typical intensity-modulated radiation therapy (IMRT) process guided by a treatment planning system (TPS) was applied.

2. Experimental methods

The dosimeter system used in this work is shown in Fig. 1. A USB-A substrate and a microcomputer (mbed LPC11U24, NXP, Eindhoven, Netherlands) dock were employed to measure the capacitor charging and

* Corresponding author.
E-mail address: syamagu@iwate-med.ac.jp (S. Yamaguchi).

https://doi.org/10.1016/j.physo.2020.100026
Received 25 March 2020; Received in revised form 10 June 2020; Accepted 13 June 2020
Available online 21 June 2020

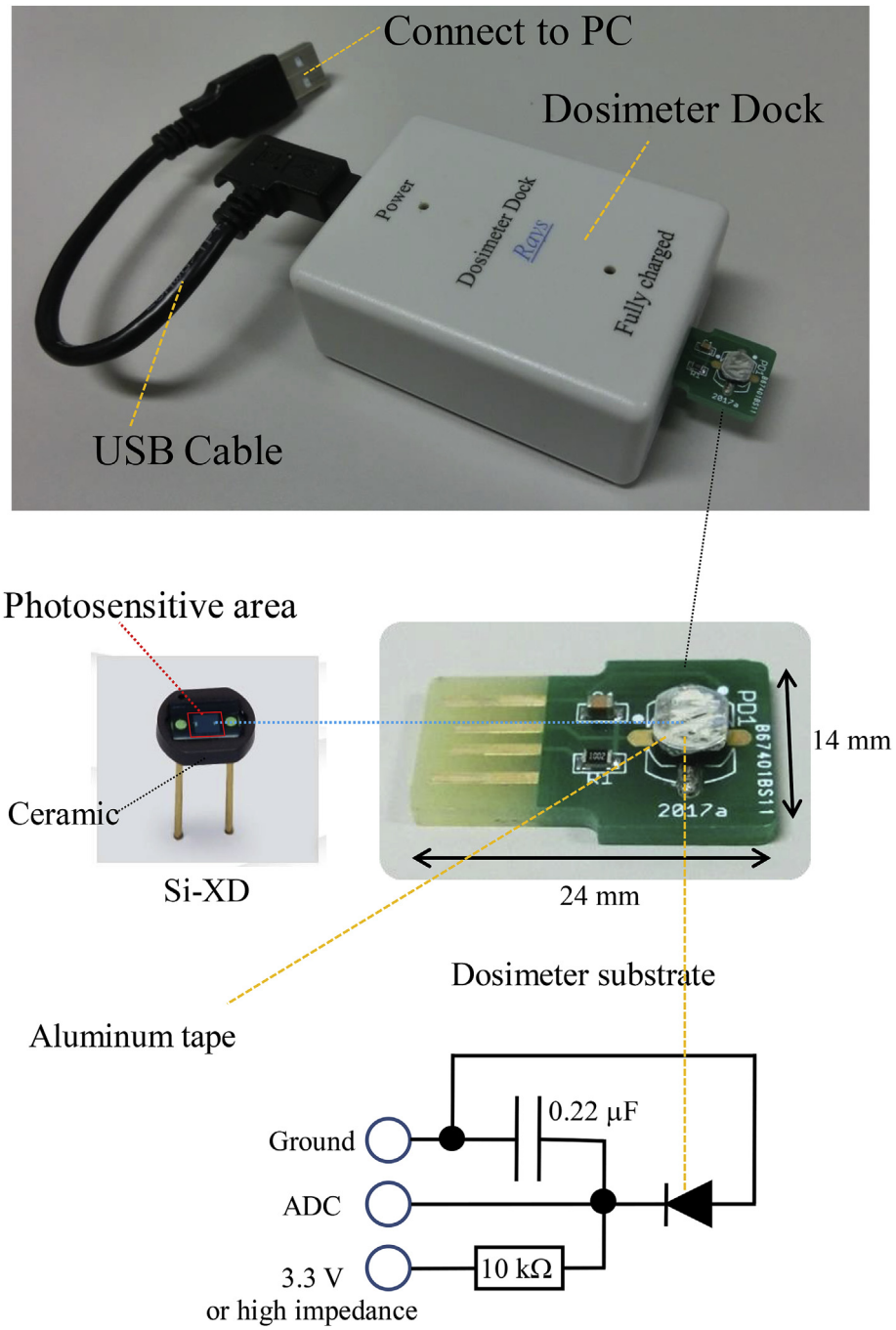

Fig. 1. Capacitor dosimeter consisting of a microcomputer dock and a substrate.

discharging voltages. The substrate was designed to insulate the patient's skin from the electrical circuit, and had a 0.22-μF capacitor (RS No. 111-0072, TDK, Tokyo, Japan), an Si-XD (S1087-01, Hamamatsu Photonics K.K., Hamamatsu, Japan) with photosensitive dimensions of 1.3 × 1.3 mm^2, and a 10-kΩ resistor. The photosensitive area was shaded using a 25-μm-thick aluminum tape, and the X-rays passing through the tape were detected using the Si-XD.

The substrate was first inserted into the dock, and the capacitor in the substrate was charged to 3.30 V. The capacitor charging voltage was measured using an analog-to-digital converter (ADC). After charging, the substrate was then removed from the dock and placed at the measurement point. While the X-rays are irradiated with a linac, the capacitor was discharged by the photocurrent flowing through the Si-XD diode. The capacitor discharging voltage was measured by re-inserting the substrate into the dock, and the voltage was measured with the ADC located in the dock. The dock was connected to a personal computer (PC) through a USB cable, to record the capacitor charging and discharging voltages.

To convert the discharging voltage into a dose, a dose calibration using a typically available ionization chamber and a phantom are needed. In this study, a Farmer-type ionization chamber (N30013, PTW, Freiburg, Germany), an electrometer (RAMTEC Smart, Toyo Medic, Tokyo, Japan) and a solid-water phantom slab (WD, Kyoto Kagaku, Kyoto, Japan) with a physical density of 1020 kg/m^3 as a water-equivalent phantom was used. The experimental setup for dose calibration using a substrate is shown in Fig. 2. A linac (Clinac iX, Varian Medical Systems, Palo Alto, CA, USA) was used to produce a 4-MV X-ray beam with outputs ranging from 25 to 250 monitor unit (MU) at a rate of

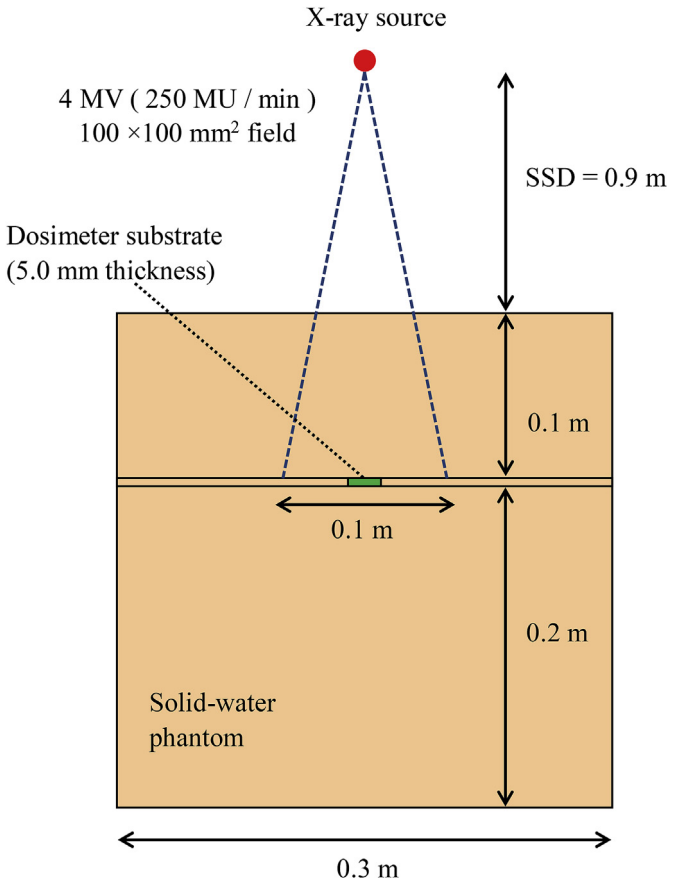

Fig. 2. Experimental setup around a solid-water phantom. 1020 kg/m^3.

250 MU/min, with an irradiation-field of 100 × 100 mm^2. The X-ray dose was measured by placing the Si-XD surface of the 5-mm-thick substrate at a depth of 0.1 m in the solid-water phantom slab, and the source-to-surface distance (SSD) was set to 0.9 m. We used one substrate and repeated the three times each measurement. Next, the standard-absolute dose was measured with the Farmer-type ionization chamber under conditions identical to those used with substrate measurements.

After the dose calibration, surface dose measurement was carried out using a custom-made head-neck phantom, also with a physical density of 1020 kg/m^3.

Fig. 3 shows the surface dose measurement methods. The dose distribution was calculated with an X-ray CT (Optima CT580, GE Healthcare, Chicago, USA), conducted with the head-neck phantom at a slice thickness of 1.25 mm and a tube voltage of 120 kV. The treatment planning system was the Eclipse (Ver. 11, Varian Medical Systems, Palo Alto, CA, USA), and the anisotropic analytic algorithm (AAA) with a matrix size of 2.5 mm was used to calculate the dose. Three planning target volumes (PTVs) were virtually created in the TPS [Fig. 3(a)], and nine fields at 4-MV X-ray beams with fixed gantry angles (75, 110, 130, 155, 180, 205, 230, 250, and 285°) were used for the IMRT planning. The IMRT was planned with simultaneous-integrated boost (SIB). The prescribed average dose of 30 fractions in PTV1, PTV2, and PTV3 were 66, 60, and 54 Gy, respectively.

Five substrates with Si-XD were placed at five different locations on the head-neck phantom surface, and an X-ray CT was conducted at a slice thickness of 1.25 mm and a tube voltage of 120 kV. A dose measurement plan for one fraction was created from the IMRT plan by transferring the beam data into the newly conducted X-ray CT. Fig. 3 (b) shows the dose measurement plan using the head-neck phantom and Si-XD. S1–S5 indicate the five Si-XD locations determined with newly conducted X-ray CT. The Si-XD contours were accurately determined from the position of the 3D-CT image. The dose-volume histograms (DVHs) were calculated by utilizing the TPS.

The DVHs at the five Si-XD locations are shown in Fig. 4, with S3 showing the highest dose among the five locations, since it was located in PTV1. In comparison, S1 showed the lowest dose due to its location outside the irradiation region. The S4 and S5 dose are lower than the S3 dose, since S5 was located near PTV1, and S4 was located in PTV2. The S2 location displayed a lower dose than S4 and S5, since it is farther from PTV1 and PTV2. In this study, the 2%-volume dose $D_{2\%}$, and the average dose D_{mean} were calculated from the DVHs.

The five substrates were placed at each surface location and measured three times. The dose difference D_d (%) was evaluated with the following equation:

$$D_d = \frac{(D_c - D_a)}{D_a} \times 100$$

where D_c is the TPS dose ($D_{2\%}$, D_{mean}) and D_a is the substrate dose.

In addition, to measuring the dose in PTV1 region corresponding to the dose of one fraction as a reference, a Farmer-type ionization chamber (N30013, PTW, Freiburg, Germany) was inserted at 65 mm from isocenter in the head direction and measured once.

3. Results

The standard absorbed dose measured at a depth of 0.1 m in the solid-water phantom is shown in Fig. 5 (a). The measured dose was proportional to the MU level, and the maximum dose at 250 MU was 1.82 Gy. The absolute dose using the substrate was determined from this result.

The MU dependence on the capacitor charging voltages is presented in Fig. 5 (b). The SDs is described on the right vertical axis in Fig. 5 (b). The maximum SD was 4.0 × 10^{-3} V. Therefore, the capacitor discharging voltages were relatively stable, affirming that dose measurement could be performed. The charging voltage decreased with increasing MU. It is important to determine the initial charging voltage correctly before capacitor discharging, because the initial voltage decreases slightly after removing the substrate from dosimeter dock, due to the input impedance of the ADC in the dock. In this experiment, the initial charging voltage at 0 MU was 3.27 V.

The converted dose calculated from the capacitor discharging voltages with changes in the MU is shown in Fig. 5 (c). The absolute dose value was determined by one-point calibration using a maximum value of 1.82 Gy at 250 MU. The dose increased in proportion to the increase in MU, and the calibrated dose were almost equivalent to those shown in Fig. 5 (a).

The relationship between the capacitor charging voltages, and the dose using the capacitor dosimeter at five different locations on the head-neck phantom are shown in Fig. 6 (a) and 6 (b), respectively. The capacitor voltage decreased significantly on the neck portion, and the dose was higher than on the head portion.

Table 1 shows the measured dose using the capacitor dosimeter, and the calculated dose using TPS at five locations.

The dosimetric comparisons using D_d are shown in Fig. 7. The D_d values exceeding 40% were at S1, because this location was outside the irradiation field. Although the D_{mean} values of TPS were lower than the measured dose, the $D_{2\%}$ values were higher than the same at the S2 to S5 locations.

It has been reported that the dose-calculation accuracy for the outside field is relatively low in the TPS [12,13]. In this study, the measured dose at S1 in Fig. 7, around the eyes on the head-neck phantom were higher than the calculated values from the TPS. Therefore, it may be useful to monitor the dose around eye lenses using the substrates.

On the other hand, the measured dose at the S2 to S5 locations were between the D_{mean} and $D_{2\%}$ values in Fig. 7. Because the size of the Si-XD is 1.3 × 1.3 mm^2, slight changes in the substrate position caused differences from the TPS in the dose comparisons. In addition, the grid size

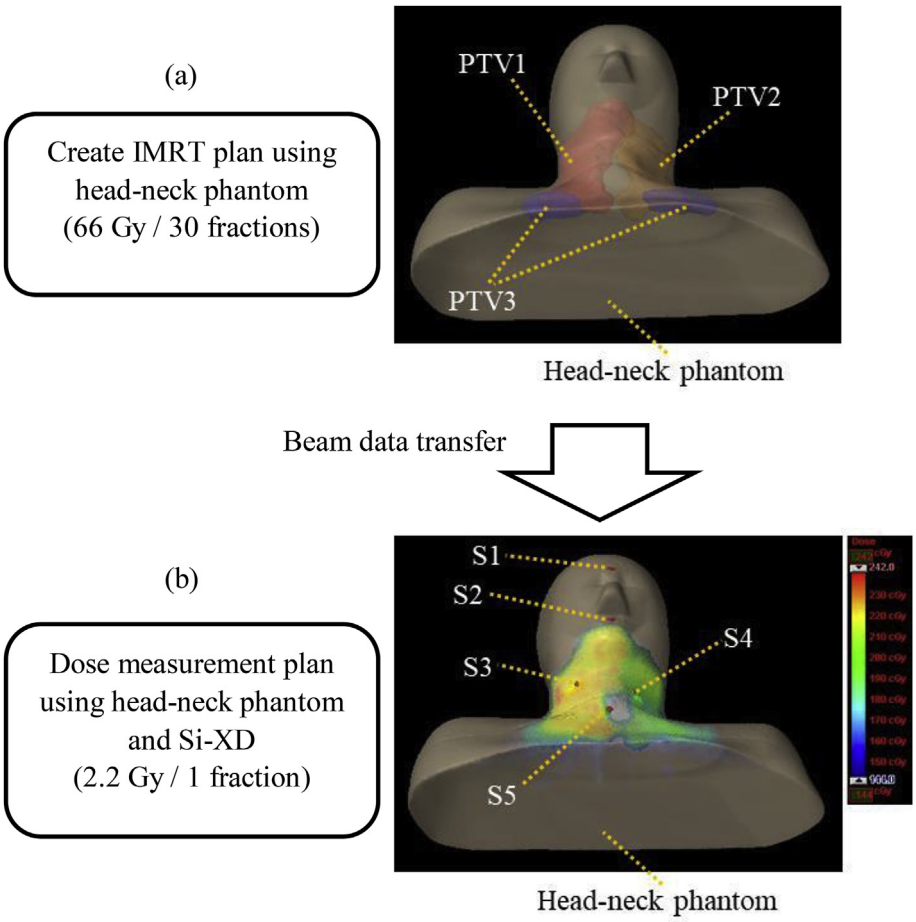

Fig. 3. Methods of surface dose measurement using a head-neck phantom: (a) Intensity-modulated radiation therapy (IMRT) plan, (b) dose measurement plan; S1 to S5 indicate the five locations of the Si-XD on the surface of the head-neck phantom.

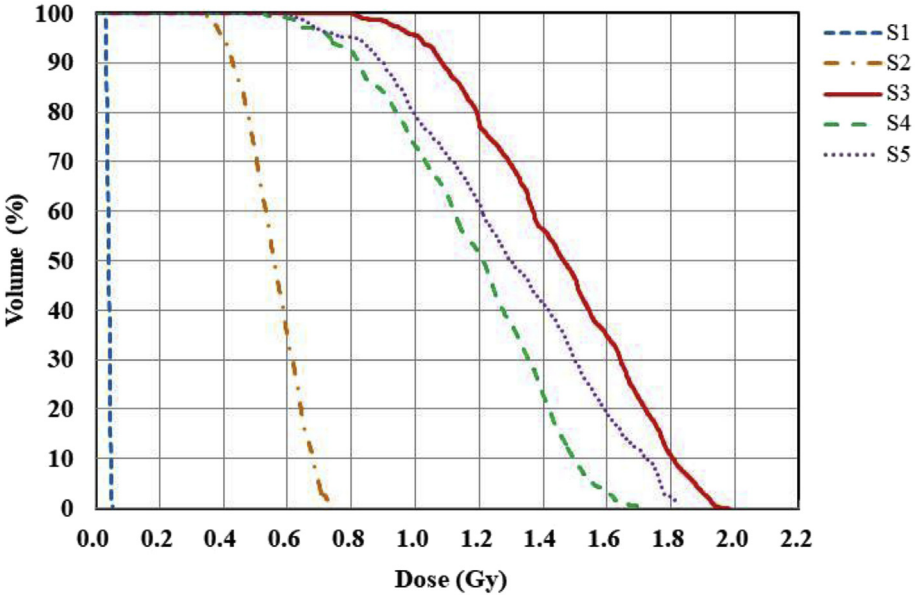

Fig. 4. Dose-volume histograms of the silicon X-ray diode at the locations of five substrates. (For interpretation of the references to colour in this figure legend, the reader is referred to the Web version of this article.)

influence on dose calculation by volume effect might be relevant. In this experiment, 2.5 mm was selected as the matrix size for dose calculation, which is as typically used in clinical facilities. This value also depends on the dose calculation algorithm, and the required corrections [14–17].

It is necessary to consider the dose calibration method on the phantom surface in order to measure dose with high accuracy. However,

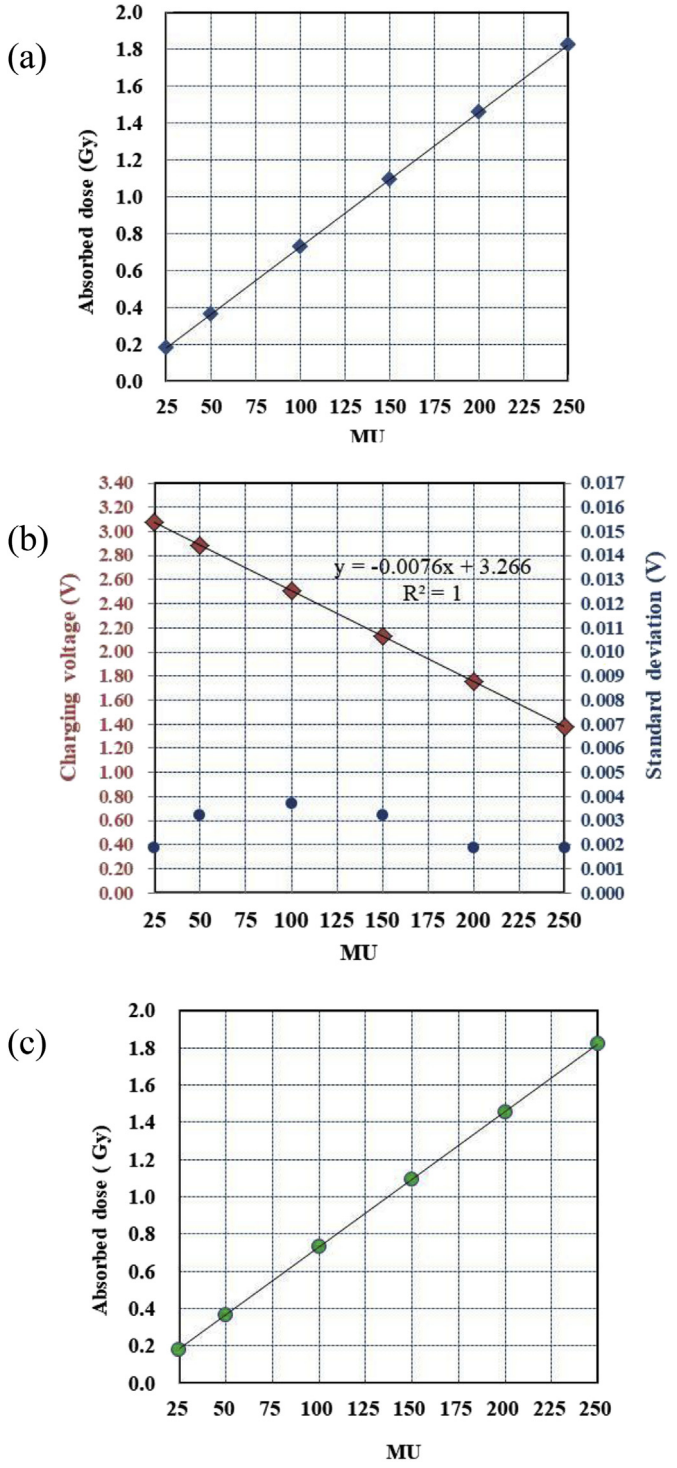

Fig. 5. Relationship between the charging voltage and the dose. (a) MU dependence of the dose measured using an ionization chamber. (b) Capacitor charging voltages versus MU after X-ray irradiation and (c) MU dependence of the dose determined by one-point calibration.

surface dosimetry using an ionization chamber is yet to be standardized; therefore, further studies are needed to confirm a phantom surface-dose calibration method using the substrate.

In general, the dose measured with the substrate and the Si-XD were proportional to the MU for the 4-MV X-ray beam, and the calibrated dose was almost equivalent to those measured with a Farmer-type ionization chamber, with small SDs. Therefore, one-point calibration was optimal to determine the dose in this study.

As a reference, a dose measurement was performed with a Farmer-type ionization chamber placed inside the head-neck phantom. The

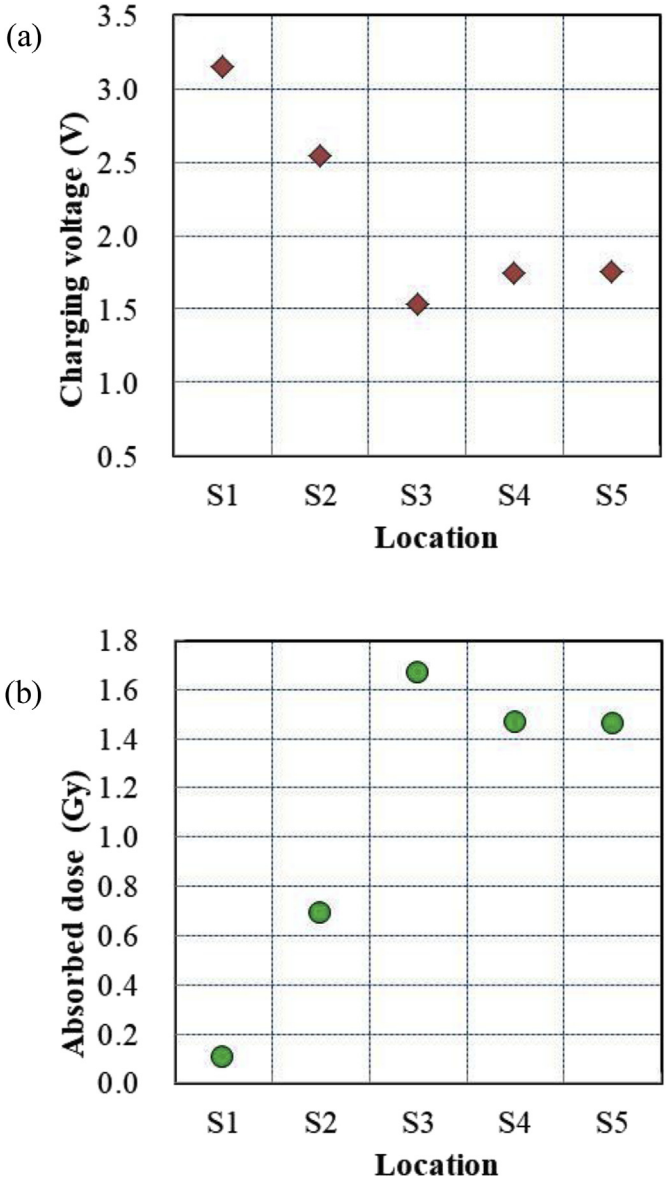

Fig. 6. Capacitor charging voltages and dose after X-ray irradiation to the head-neck phantom by intensity-modulated radiation therapy at five locations. (a) Capacitor charging voltages, and (b) dose calculated from the capacitor discharging voltages using one-point calibration.

Table 1
Measured dose using the substrates and the head-neck phantom determined by one-point calibration, and the calculated dose by the treatment planning system at five locations.

Location	Substrate Dose (Gy) Average ± SD	TPS($D_{2\%}$) Dose (Gy)	TPS(D_{mean}) Dose (Gy)
S1	0.11 ± 0.004	0.05	0.04
S2	0.69 ± 0.002	0.72	0.56
S3	1.67 ± 0.002	1.92	1.45
S4	1.47 ± 0.004	1.62	1.18
S5	1.46 ± 0.002	1.81	1.30

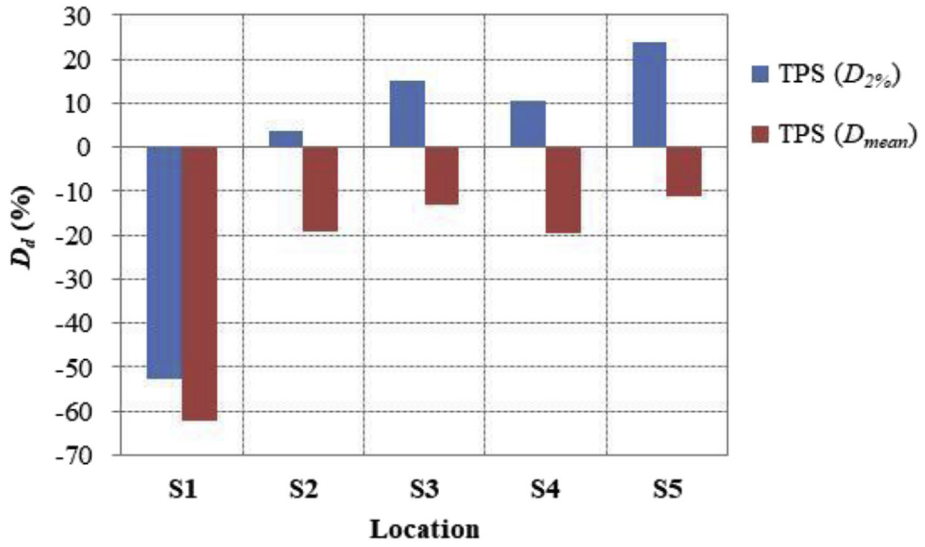

Fig. 7. Dosimetric comparisons using D_d at the indicated locations. D_d values exceeding 40% were seen at S1.

measured dose was 2.23 Gy using the ionization chamber, and the calculated dose in TPS was 2.27 Gy. Therefore, the D_d values was 1.83%; the resulting dose difference was less than the differences between the measurements on the phantom surface.

To prevent self-discharging of the capacitor, the dose should be promptly measured after X-ray irradiation. Thus, the development of a compact dock is useful for measuring the dose immediately and for reducing the cost of the dosimeter. In addition, the sensitivity at the planned dose can be optimized by the capacitance.

The bolus effect of the dosimeter alone, and its influence on the dose distribution in the body, must be considered before using this dosimeter in the irradiation field. Also, if the Si-XD height in the substrate is 5 mm, it is difficult to measure the patient-skin dose directly using this substrate. However, the measured dose using the substrate will be proportional to the patient-skin dose; it will be useful to monitor the changing skin dose during the course of radiation therapy.

4. Conclusions

A low-price capacitor dosimeter was developed, consisting of a dosimeter dock, and a surface-mounted USB-A substrate with a Si-XD; the cost of the substrate is about 10 US$. The decrease in the capacitor charging voltage was shown to be proportional to the X-ray dose from a medical linear accelerator, and the calibrated dose corresponded well to that measured using a Farmer-type ionization chamber, with small standard deviations. The results suggest that the capacitor dosimeter is useful for monitoring patient-surface dose during radiation therapy.

Declaration of competing interest

The authors declare that they have no known competing financial interests or personal relationships that could have appeared to influence the work reported in this paper.

CRediT authorship contribution statement

Satoshi Yamaguchi: Writing - original draft. **Eiichi Sato:** Writing - review & editing. **Yoshiro Ieko:** Visualization, Investigation. **Hisanori Ariga:** Supervision. **Kunihiro Yoshioka:** Supervision.

Acknowledgements

This work was supported by Grants from Keiryo Research Foundation, Promotion and Mutual Aid Corporation for Private Schools of Japan, Japan Science and Technology Agency (JST), and JSPS KAKENHI (17K10371, 17K09068, 17K01424, 17H00607). This study was also supported by a Grant-in-Aid for Strategic Medical Science Research (S1491001, 2014–2018) from the Ministry of Education, Culture, Sports, Science and Technology of Japan.

References

[1] N. Lee, C. Chuang, J.M. Quivey, T.L. Phillips, P. Akazawa, L.J. Verhey, P. Xia, Skin toxicity due to intensity-modulated radiotherapy for head-and-neck carcinoma, Int. J. Radiat. Oncol. Biol. Phys. 53 (3) (2002) 630–637.
[2] K. Eric, M. Kara Bucci, M Quivey Jeanne, Vivian Weingerg, Ping Xia, Repeat CT imaging and replanning during the course of IMRT for head-and-neck cancer, Int. J. Radiat. Oncol. Biol. Phys. 64 (2) (2006) 355–362.
[3] M.A. Deveau, A.N. Gutierrez, T.R. Mackie, W.A. Tome, L.J. Forrest, Dosimetric impact of daily setup variations during treatment of canine nasal tumors using intensity-modulated radiation therapy, Vet. Radiol. Ultrasound 51 (1) (2010) 90–96.
[4] Y. Gu, H. Yu, X. Zuo, Q. Cao, T. Liang, Y. Ren, H. Yang, D. Yang, Comparisons of skin toxicity in patients with extranodal nasal-type natural killer/T-cell lymphoma after treatment with intensity-modulated radiotherapy and conventional radiotherapy, J. Canc. Res. Therapeut. 14 (Supplement) (2018) S975–S979.
[5] Y. Jihyung, X. Yibo, X. Rui, Evaluation of surface and shallow depth dose reductions using a Superflab bolus during conventional and advanced external beam radiotherapy, J. Appl. Clin. Med. Phys. 19 (2) (2018) 137–143.
[6] L. Coppeta, A. Pietroiusti, A. Neri, A. Spataro, E. De Angelis, S. Perrone, A. Magrini, Risk of radiation-induced lens opacities among surgeons and interventional medical staff, Radiol. Phys. Technol. 12 (1) (2019) 26–29.
[7] S.M. Nguyen, J. Sison, M. Jones, J.L. Berry, J.W. Kim, A.L. Murphree, V. Salinas, A.J. Olch, E.L. Chang, K.K. Wong, Lens dose-response prediction modeling and cataract incidence in retinoblastoma patients after lens-sparing or whole-eye radiotherapy, Int. J. Radiat. Oncol. Biol. Phys. 103 (5) (2019) 1143–1150.
[8] T.A. Reynolds, P. Higgins, Surface dose measurements with commonly used detector: a consistent thickness correction method, J. Appl. Clin. Med. Phys. 16 (5) (2015) 358–366.
[9] S. Yamaguchi, E. Sato, R. Nakamura, H. Oikawa, H. Kakuhara, K. Kikuchi, H. Ariga, S. Ehara, Disposable capacitor dosimeter using a skin-insulated mini-substrate with a silicon X-ray diode in image-guided radiation therapy, Int. J. Med. Phys. Clin. Eng. Radiat. Oncol. 7 (1) (2018) 35–46.
[10] S. Yamaguchi, E. Sato, Product development of a capacitor dosimeter using a skin-insulated USB-A-substrate with a silicon X-ray diode, Radiol. Phys. Technol. 12 (1) (2019) 69–75.
[11] Y. Arakawa, E. Sato, H. Kogita, T. Hamaya, S. Nihei, W. Numahata, S. Kami, Y. Oda, O. Hagiwara, H. Matsukiyo, A. Osawa, T. Enomoto, M. Watanabe, S. Kusachi, S. Sato, A. Ogawa, Investigation of X-ray photon-counting using ceramic-substrate silicon diode and its application to gadolinium imaging, Jpn. J. Appl. Phys. 53 (7) (2014), 072201-1-5.

[12] K. Wijesooriya, N.K. Liyanage, M. Kaluarachchi, D. Sawkey, Part II: verification of the TrueBeam head shielding model in Varian VirtuaLinac via out-of-field doses, Med. Phys. 46 (2) (2019) 877–884.
[13] R. Harrison, Out-of-field doses in radiotherapy: input to epidemiological studies and dose-risk models, Phys. Med. 42 (2017) 239–246.
[14] O. Ryota, A. Fujio, O. Takeshi, N. Yuji, K. Yudai, T. Yuuki, H. Kazunari, Accuracy of dose calculation algorithms for virtual heterogeneous phantoms and intensity-modulated radiation therapy in the head and neck, Radiol. Phys. Technol. 9 (1) (2016) 77–87.
[15] S. Devic, J. Seuntjens, W. Abdel-Rahman, M. Evans, M. Olivares, E.B. Podgorsak, T. Vuong, C.G. Soares, Accurate skin dose measurements using radiochromic film in clinical applications, Med. Phys. 33 (4) (2006) 1116–1124.
[16] M. Nakano, R.F. Hill, M. Whitaker, J.H. Kim, Z. Kuncic, A study of surface dosimetry for breast cancer radiotherapy treatments using Gafchromic EBT2 film, J. Appl. Clin. Med. Phys. 13 (3) (2012) 3727.
[17] L.E. Court, R. Tishler, H. Xiang, A.M. Allen, M. Makrigiorgos, L. Chin, Experimental evaluation of the accuracy of skin dose calculation for a commercial treatment planning system, J. Appl. Clin. Med. Phys. 9 (1) (2008) 2792.